

Low-insertion-loss femtosecond laser-inscribed three-dimensional high-density mux/demux devices

Yize Liang,^{a,b,c,†} Chengkun Cai^{Ⓞ, a,b,c,†} Kangrui Wang,^{a,b,c} Xiaokang Lian,^{a,b,c} Jue Wang,^{a,b,c} Jinfeng Liu,^{a,b,c} Lei Shen,^d and Jian Wang^{a,b,c,*}

^aHuazhong University of Science and Technology, Wuhan National Laboratory for Optoelectronics and School of Optical and Electronic Information, Wuhan, China

^bOptics Valley Laboratory, Wuhan, China

^cShenzhen Institute of Huazhong University of Science and Technology, Shenzhen, China

^dYangtze Optical Fiber and Cable Joint Stock Limited Company (YOFC), State Key Laboratory of Optical Fiber and Cable Manufacture Technology, Wuhan, China

Abstract. Recently, transmitting diverse signals in different cores of a multicore fiber (MCF) has greatly improved the communication capacity of a single fiber. In such an MCF-based communication system, mux/demux devices with broad bandwidth are of great significance. In this work, we design and fabricate a 19-channel mux/demux device based on femtosecond laser direct writing. The fabricated mux/demux device possesses an average insertion loss of 0.88 dB and intercore crosstalk of no more than -29.1 dB. Moreover, the fabricated mux/demux device features a broad bandwidth across the C+L band. Such a mux/demux device enables low-loss 19-core fiber (de)multiplexing over the whole C+L band, showing a convincing potential value in wavelength-space division multiplexing applications. In addition, a 19-core fiber fan-in/fan-out system is also established based on a pair of mux/demux devices in this work.

Keywords: femtosecond laser direct writing; space-division multiplexing; mux/demux device; multicore fiber.

Received Jan. 16, 2023; revised manuscript received Feb. 27, 2023; accepted for publication Mar. 9, 2023; published online Apr. 12, 2023.

© The Authors. Published by SPIE and CLP under a Creative Commons Attribution 4.0 International License. Distribution or reproduction of this work in whole or in part requires full attribution of the original publication, including its DOI.

[DOI: [10.1117/1.APN.2.3.036002](https://doi.org/10.1117/1.APN.2.3.036002)]

1 Introduction

Over the last couple of years, the communication capacity of single-mode fiber (SMF)-based systems has been rapidly pushed toward its theoretical limit¹ due to the explosive growth in demand for optical communication traffic. Thus, space-division multiplexing (SDM) has been proposed and demonstrated to be a promising technology to further increase the capacity of a single optical fiber.^{2,3} There are currently two kinds of fiber-based SDM communication systems. One propagates orthogonal spatial modes loaded with different signals in the single core of a multimode fiber⁴⁻⁷ and the other transmits different signals in diverse cores of a multicore fiber (MCF).⁸⁻¹⁴

Remarkably, high communication capacities with long-distance transmission have been accomplished by applying SDM transmission in MCFs. For instance, 2.15 Pb/s transmission was demonstrated applying a 22-core homogeneous single-mode MCF and a wideband optical comb.¹⁰ 105.1 Tb/s, 14,350-km transmission was achieved using a 12-core MCF.¹⁵

One important component for such an MCF-based SDM system is a fan-in/fan-out (FIFO) device with broad bandwidth, low insertion loss, and low crosstalk, which acts as an SDM mux/demux device. With the development of MCF-based SDM technology, several kinds of FIFO devices have been proposed and fabricated. Generally speaking, they can be divided into three kinds: traditional free-space FIFO couplers,^{16,17} fiber-based FIFO couplers,¹⁸⁻²¹ and on-chip FIFO couplers.²²⁻²⁸ Traditional free-space FIFO couplers based on free-space optical devices have been widely utilized owing to their high efficiencies.

*Address all correspondence to Jian Wang, jwang@hust.edu.cn

[†]These authors contributed equally to this work.

However, they are too bulky. Fiber-based FIFO couplers can be divided into two kinds: tapered MCF connectors^{18,19} and etched fiber bundles.^{20,21} Such two kinds of fiber-based couplers feature low insertion loss, small size, and low crosstalk. Thus, they are capable of transmitting different signals in different spatial channels in long-haul MCFs. Compared to these methods, on-chip FIFO solutions are also preferred because, from an integration point of view, other functionalities can be integrated with them. Several kinds of integrated FIFO chips based on different platforms have been reported, such as on-chip grating coupler arrays on silicon-on-insulator (SOI) platforms^{22,23} and silicon nitride platforms,²⁴ FIFO polymer waveguides,^{25,26} and ultrafast laser-inscribed FIFO waveguides based on glass platforms.^{27,28} Among them, inscribing waveguides in a glass chip is a competitive solution,^{29–31} possessing the characteristics of low cost and broad bandwidth. Unfortunately, as the number of channels increases, the inside of the device will be more crowded, which will lead to a higher bend loss. A longer length of the device will provide more space; however, it means a higher path loss. Thus, a reasonable design of the device is of great significance because it aims to minimize the sum of path loss and bending loss. Moreover, a high-performance light-field matching of device and commercial SMF array also affects the loss.

In this work, we design and fabricate 19-channel FIFO devices based on femtosecond laser direct writing. The insertion losses of 19 channels are evaluated to be no more than 1.2 dB at 1550 nm with an average value of 0.88 dB. In addition, insertion losses of specific channels are characterized to be almost the same over the whole C+L band, proving the broad bandwidth of this FIFO device. Intercore crosstalk of the FIFO device is also evaluated to be no more than -29.1 dB. Applying a pair of FIFO devices and a 1-km 19-core fiber, a 19-core fiber FIFO system is established. Remarkably, such a femtosecond laser-inscribed 19-channel FIFO device, which features low insertion loss, broad bandwidth, and low crosstalk, may be able to promote applications in different areas, such as long-haul SDM data transmission,^{8–14} quantum information processing,^{32,33} MCF-based sensing,^{34,35} and imaging.^{36,37}

2 Results

2.1 Design and Fabrication of the FIFO Device

Figure 1(a) displays the schematic of the femtosecond laser direct writing system. The glass sample (20 mm \times 50 mm \times 1 mm) is

placed on a three-dimensional stage. The femtosecond laser beam is tailored by a slit and then vertically focused into the sample through a 50 \times objective (NA = 0.42). The FIFO device is fabricated along the 20-mm side. Utilizing an LED lighting system and a visible CCD, the femtosecond laser direct writing process is monitored in real time. During the fabricating process, the glass sample is translated using a high precision XYZ air-bearing stage. The femtosecond laser beam is tailored by a slit so that approximately circular cross sections can be formed on the end facet of the glass. An approximately circular shape of the FIFO waveguide cross section will promote the mode field match between the FIFO device and 19-core fiber.³⁸ Moreover, through adjusting the parameters of the femtosecond laser direct writing system, the size of the approximately circular cross sections is adjusted so that high-performance light-field matching of the SMF array and the device can be achieved. As a result, the coupling loss will also be lower. (More details and parameters of the fabrication process can be found in Table S1 in the [Supplemental Material](#).)

For traditional ultrafast laser-inscribed FIFO devices fabricated in quartz glass, they are usually fabricated in the thermal fabrication regime (e.g., 5.1-MHz ultrafast laser). In such regimes, cumulative effects take place. The low pulse energy of the applied high-frequency lasers requires a high NA objective lens to achieve a few-hundred micrometers' vertical fabrication range. In these regimes, modifications are of a circular cross section due to the isotropic heat diffusion. In contrast, we choose a low-frequency (100 kHz) laser to accomplish the material modification produced by the individual pulses. The applied low NA objective lens enables the vertical fabrication range up to a few micrometers. Thus, waveguides inscribed in low-frequency regimes usually exhibit significant loss and strong core asymmetry with a large aspect ratio. However, we apply the slit beam shaping technique to fabricate waveguides with a circular cross section and low loss over a large depth range. In addition, the main parameters of the fabrication process are scanned, and the comprehensive optimal value is selected. In this way, we achieve both the ultralow propagation loss (~ 0.1 dB/cm) and high mode field matching performance of quartz glass FIFO devices.

The concept of a fabricated 19-channel FIFO device is indicated in Fig. 1(b). A side-by-side 19-channel Gaussian beam array that outputs from a SMF array is incident into the FIFO device. As a result, different beams of the beam array are confined to transmit along different channels in the FIFO

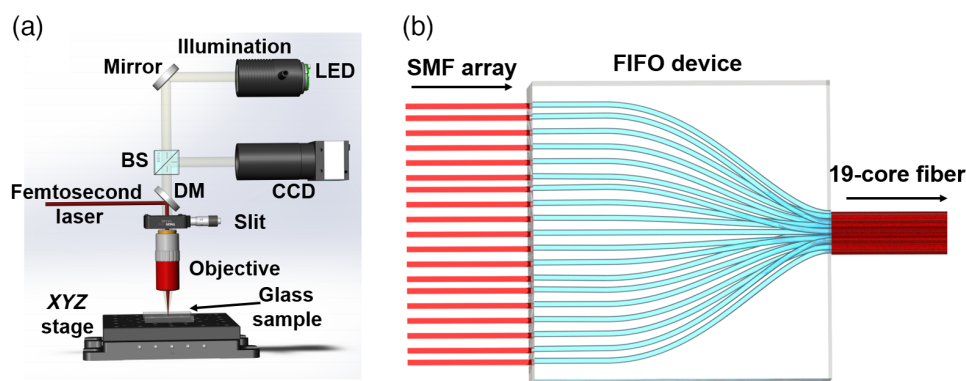


Fig. 1 (a) Schematic of the femtosecond laser direct writing system and (b) concept of the femtosecond laser-inscribed device. BS, beam splitter; DM, dichroic mirror; CCD, charge-coupled device.

device. The transmission of different beams in their corresponding channels is, in other words, a process of beam array redistribution in three dimensions. The redistributed beam array forms a distribution that matches a 19-core fiber. Therefore, light beams output from a SMF array can be accurately coupled into diverse cores of a 19-core fiber, as displayed in Fig. 1(b). By modulating different signals onto different beams transmitting in the SMF array, such a 19-channel FIFO device can be used as an SDM multiplexer that connects a commercial SMF array and a 19-core fiber.

Figure 2(a) shows the designed end facets of the input and output of the 19-channel FIFO device, while Fig. 2(b) shows the captured output end facet by applying a microscope. The side-by-side channel distribution at the input of the FIFO device possesses a channel spacing of $127\ \mu\text{m}$ to match a commercial SMF array. The channel distribution at the output end corresponds to the core distribution of a 19-core fiber so that light beams output from the FIFO device can be coupled into the 19-core fiber with high efficiency. To clarify the corresponding relationship between the input channels and output channels of the FIFO device, we number the channels of the FIFO device from 1 to 19, as displayed in Fig. 2(a). Figure 2(c) shows the captured cross section of the utilized 19-core fiber with size information marked.

The fundamental principle for fabricating such a 19-channel FIFO device relies on the direct writing of 19 waveguides in glass. The 19 waveguides inside the FIFO device get closer to each other along the track from its input to output, as

indicated in Fig. 1(b). In what follows, we explain the design of the FIFO device in detail.

First, the design of the input and output channel distribution of the 19-channel FIFO device is required. The channel spacing of the input end of FIFO device is set to be $127\ \mu\text{m}$ to match the distribution of applied SMF array. The channel distribution of the output end of the FIFO device is required to match the core distribution of the applied 19-core fiber. Figure 2(c) shows the captured cross section of the applied 19-core fiber, which possesses a $9\text{-}\mu\text{m}$ core diameter and a $125.32\text{-}\mu\text{m}$ cladding radius. The 19 cores can be divided into three types of cores located in three concentric circles: that is, one core in the middle of fiber, six cores in the second circle, and 12 cores in the third circle. A $42.655\text{-}\mu\text{m}$ spacing exists between adjacent cores in the second circle, while a $44.16\text{-}\mu\text{m}$ spacing exists between adjacent cores in the third circle. In addition, a $42.655\text{-}\mu\text{m}$ spacing exists between the middle core and cores in the second circle. An $85.31\text{-}\mu\text{m}$ spacing exists between the middle core and cores in the third circle.

After finishing the design of the input and output channel distributions of the 19-channel FIFO device, tracks of the 19 waveguides inside the FIFO device should be determined, with the principle of independent transmission. Ultraviolet (UV) optical quartz glass with a size of $20\ \text{mm} \times 50\ \text{mm} \times 1\ \text{mm}$ is utilized as the substrate material. Its 20-mm side is chosen as the waveguide length. The channel number of input end facet and output end facet is shown in Fig. 2(a). The channel 10 here is set as a straight waveguide, while other channels are designed to be

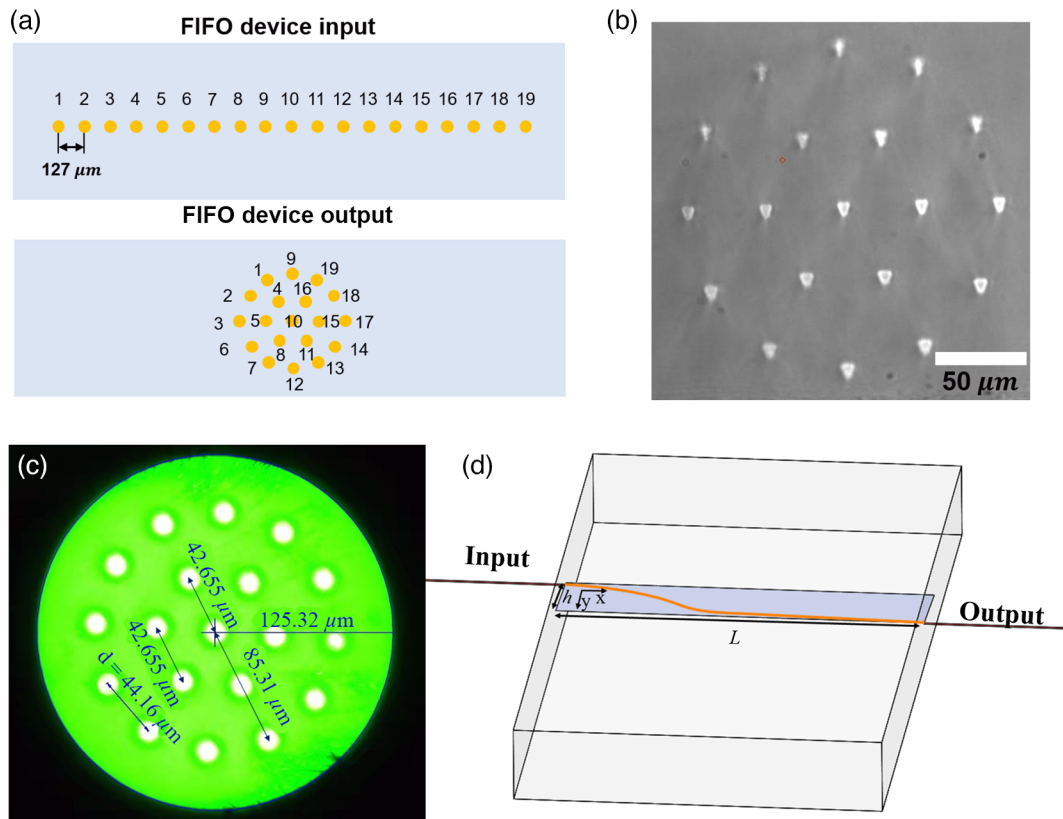


Fig. 2 (a) Design of the input end facet and output end facet of the FIFO device; (b) captured output end facet of the FIFO device; (c) captured cross section of applied 19-core fiber; and (d) design of the 2D track of the waveguide.

bending waveguides. Tracks of 18 bending channels should be designed obeying the following rules: (i) confirm the plane on which the track is located. Assuming that input and output beam of the FIFO device propagates along horizontal lines, as shown in Fig. 2(d), a specific plane is determined that contains both the input line and output line; (ii) plotting the following 2D track on this specific plane:

$$y = \frac{6h}{L^5}x^5 - \frac{15h}{L^4}x^4 + \frac{10h}{L^3}x^3, \quad (1)$$

where L denotes the horizontal length of the track, h corresponds to the vertical length of the track, and x denotes the horizontal coordinate. Then the radius of curvature of the waveguide can be expressed as

$$R = \frac{\left[1 - \frac{900h^2x^4}{L^6} \left(\frac{x}{L} - 1\right)^4\right]^{3/2}}{\frac{60hx}{L^5} \left(2\frac{x^2}{L^2} - 3\frac{x}{L} + 1\right)}, \quad (2)$$

where R denotes the radius of curvature of the waveguide. (iii) After plotting such a 2D track [like the orange track in Fig. 2(d)], one can obtain a three-dimensional track of the waveguide by considering the size of the waveguide. Thus, tracks of 19 channels are determined. To avoid shadow effects, such a fabrication sequence is utilized: channel 12 → channel 13 → channel 14 → channel 17 → channel 7 → channel 6 → channel 3 → channel 8 → channel 5 → channel 11 → channel 15 → channel 10 → channel 16 → channel 4 → channel 18 → channel 19 → channel 2 → channel 1.

2.2 Experimental Setup of 19-Channel FIFO System

To achieve the characterization of the 19-channel FIFO device, we use a pair of 19-channel FIFO devices to establish a 19-channel FIFO system. The schematic of the 19-channel FIFO system is shown in Fig. 3(a). A C+L band tunable laser is connected to

an optical coupler (OC) so that light beam output from the laser is split into 19 beams transmitting in an SMF array. The 19-channel fiber-guided beams then output from the SMF array and enter the FIFO device. During the transmission in the FIFO device, the 19-channel beam array is redistributed to form a distribution that matches the 19-core fiber. Then the 19-channel beam array is coupled into a 1-km 19-core fiber. The applied 19-core fiber possesses a measured transmission loss of 0.26 dB/km. To demultiplex the 19-channel beams output from the 1-km 19-core fiber, another FIFO device is reversely inserted into the experimental setup, as shown in Fig. 3(a). Finally, the demultiplexed side-by-side 19-channel beams that output from the FIFO device are incident into another SMF array, thereby demultiplexing the 19-channel beams into 19 different SMF channels.

In the experiment, all the coupling processes are monitored in real time by a visible CCD. To accomplish accurate coupling alignment, the two SMF arrays and the 1-km 19-core fiber are placed on six-axes stages, which enable precise control of three-dimensional angles and displacements. In addition, two rotational fiber holders are utilized to rotate the two ports of the 19-core fiber to finish the channel distribution match between the 19-core fiber and the FIFO devices. Once the 19-channel FIFO system is successfully established, all the devices (i.e., the two SMF arrays, the two FIFO devices, and the 1-km 19-core fiber) can be integrated by applying a UV glue so that the applied six-axes stages, rotational fiber holders, and monitoring CCD are freed.

2.3 Characterization of the FIFO Device

To obtain the performance of the fabricated 19-channel FIFO device, a comprehensive characterization is carried out, including capturing the output light field, measuring the insertion loss, characterizing the bandwidth, and evaluating the crosstalk of the 19-channel FIFO device.

The intensity profile of the output light field of the 19-channel FIFO device is displayed in Fig. 4(a). It is captured after

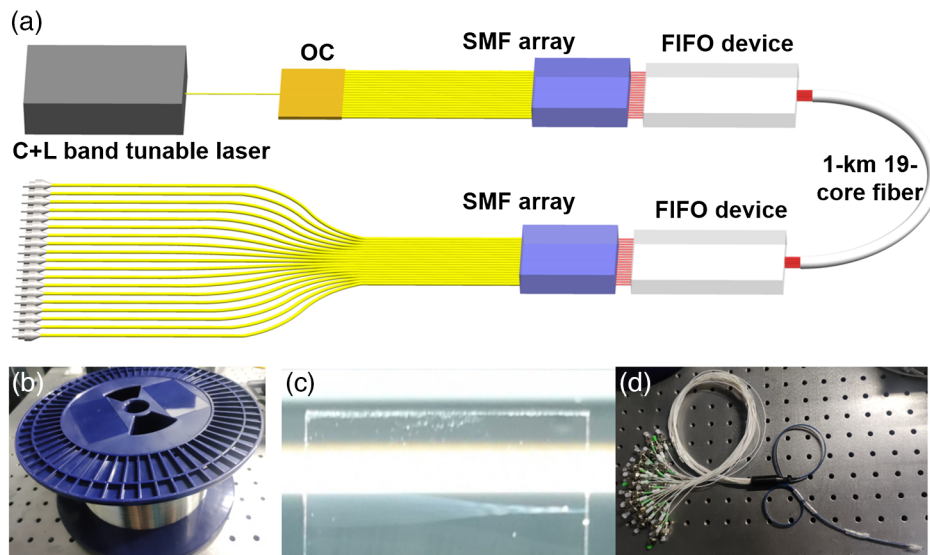


Fig. 3 (a) Experimental setup of the 19-channel FIFO system based on a pair of FIFO devices; (b) 1-km 19-core fiber; (c) 19-channel FIFO device; (d) SMF array. OC, optical coupler.

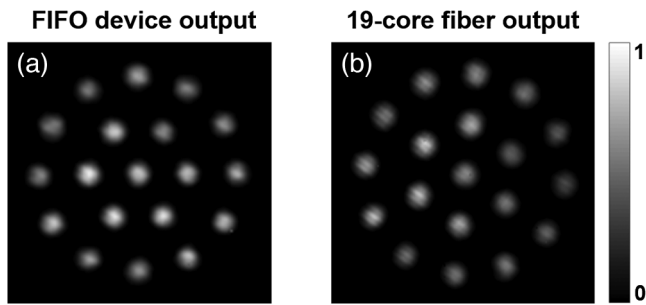


Fig. 4 Intensity profiles of the output light fields of (a) 19-channel FIFO device and (b) 1-km 19-core fiber.

the FIFO device output by using a $50\times$ objective lens and a 1550 nm CCD. Considering that all the 19 channels possess the same input power, the output intensities of 19 different channels are similar, as illustrated in Fig. 4(a). Such a uniform intensity profile proves that accurate coupling is achieved. The intensity profile of the 19-channel beam array obeys a distribution that matches the 19-core fiber, thereby coupling the 19-channel beams into a 1-km 19-core fiber. As a result, the captured intensity profile is indicated in Fig. 4(b). In Fig. 4(b), relatively obvious intensity disparity exists between different channels. This is mainly due to the imperfect coupling process. Higher-precision coupling devices (e.g., better rotational fiber holders, six-axes stages) may be a potential solution to this power disparity problem.

The insertion losses of a FIFO device result in lower received power of an SDM communication system, thereby affecting the bit error rate (BER) performance of the SDM communication system. Here, we evaluate the insertion losses of 19 different channels of the FIFO device at 1550 nm. Light beams output from the FIFO device are coupled into a short SMF for insertion loss characterization. During the loss characterizations, the input power only exists in the channel that is under test. First, the input intensity of a specific channel is measured by recording its power at the output of the OC using a fiber power meter. Then, the output intensity of this channel is measured at the output of the SMF by applying the same fiber power meter. Finally, the

insertion losses of the 19 different channels are calculated by means of subtracting the input intensities from their output intensities. The measured insertion losses of 19 different channels are evaluated to be no more than 1.2 dB at 1550 nm, which can be found in Fig. 5(a). It is worth mentioning that the measured insertion losses contain coupling losses and linear propagation loss of the FIFO waveguide. Thus, a coupling loss about 0.3 dB/facet and a linear propagation loss of about 0.1 dB/cm are evaluated for channel 10 at 1550 nm. Central channels feature lower insertion losses due to their lower bending losses and shorter paths. Compared to central channels, the low increase of channel path length of the farthest channel will not affect the insertion loss as much, due to the linear propagation loss of ~ 0.1 dB/cm. That is, the bending loss is the main reason that causes the higher insertion loss of the farthest channel.

The wavelength-division multiplexing (WDM) technology is an efficient approach to improve the optical communication capacity. Hence, the bandwidth of an SDM FIFO device is required to be large enough so that the SDM technology can be used together with WDM to further increase the capacity of the optical network. Fortunately, the fabricated 19-channel FIFO device on a glass chip has the advantage of broad bandwidth. Therefore, we measure the insertion losses of three different channels (central channel, channel 10; farther channel, channel 14; the farthest channel, channel 19) over the whole C+L band to prove it. Insertion losses of these three different channels are evaluated at diverse wavelengths from 1528 to 1625 nm with a measurement interval of 1 nm, as illustrated in Fig. 5(b). Insertion losses at different wavelengths almost retain the same value, demonstrating the C+L bandwidth of the fabricated FIFO device. Thus, the femtosecond laser-inscribed 19-channel FIFO device can be utilized as a (de)multiplexer in wavelength-space division multiplexing (WSDM) applications.

The interchannel crosstalk of an SDM system describes how much power in the input channel couples to other channels. In addition to insertion losses, the interchannel crosstalk is another factor that determines the performance of an SDM communication system. The interchannel crosstalk can be evaluated by measuring the output power of the input channel and the output power of other channels. Here, we characterize the intercore crosstalk of the 19-channel FIFO device (for details about the crosstalk characterization, refer to Fig. S1, Fig. S2, and

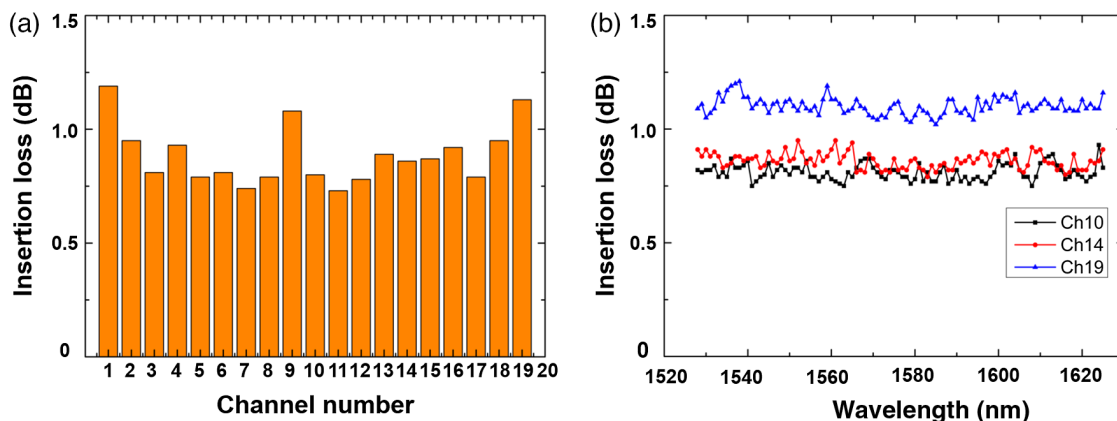


Fig. 5 (a) Measured insertion losses of 19 different channels of the FIFO device at 1550 nm and (b) evaluated insertion losses of channels 10, 14, and 19 from 1528 to 1625 nm.

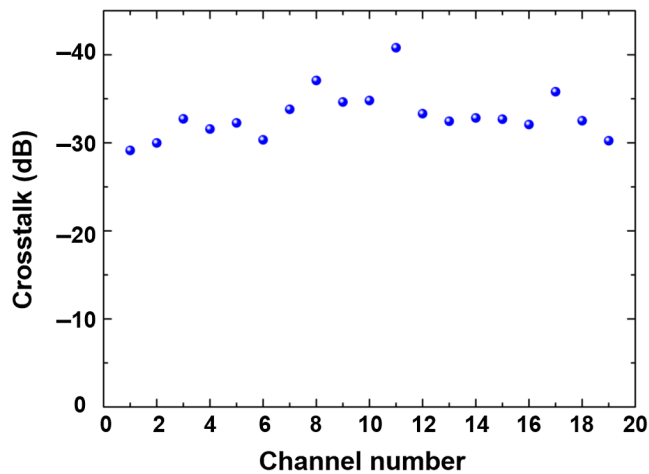


Fig. 6 Measured crosstalk of 19 different channels to other channels.

Table S2 in the [Supplemental Material](#)). For a specific channel, we choose the biggest crosstalk between it and other channels as the crosstalk of this channel, as shown in Fig. 6. All the channels possess crosstalk of no more than -29.1 dB. Such a low crosstalk enables high-speed signal transmission in a 19-core fiber.

3 Conclusion and Discussion

We designed and fabricated a 19-channel FIFO waveguide based on femtosecond laser direct writing. The insertion losses of 19 channels are evaluated to be no more than 1.2 dB at 1550 nm, with an average value of 0.88 dB. Intercore crosstalk of the FIFO device is also evaluated to be no more than -29.1 dB. In addition, the broad C+L bandwidth of the 19-channel waveguide is characterized and demonstrated by measuring the insertion losses of different channels at diverse wavelengths. Applying a pair of waveguides and 1-km 19-core fiber, a 19-core fiber FIFO system is established, showing the practical value of the fabricated FIFO device.

Compared to free-space FIFO solutions^{16,17} and fiber-based solutions,^{18,19} our FIFO mux/demux devices have the advantages of small size and low cost. In contrast to on-chip FIFO solutions based on other material platforms,^{22–26} our FIFO mux/demux devices based on glass combines the advantages of low insertion loss and broad bandwidth. Even compared to other ultrafast laser inscribing methods,^{27,28} our FIFO devices achieve the lowest propagation loss of ~ 0.1 dB/cm. Such a femtosecond laser-inscribed 19-channel FIFO device may pave the way for many applications. For instance, the FIFO device can be applied as a (de)multiplexer in large-capacity long-haul WSDM transmission based on MCF^{8–13} due to its broad bandwidth and low interchannel crosstalk. In addition, multipoint beam splitters can be achieved by a specially designed FIFO device, which is a cornerstone device for high-dimensional quantum information tasks.³⁹ Such a FIFO device is also capable of establishing integrated FIFO systems, so it may be helpful to fabricate integrated MCF-based sensors and endoscopes. In addition, a photonic lantern can also be fabricated based on femtosecond laser direct writing,^{40–45} which is desirable for SDM applications based on higher-order modes.

Acknowledgments

This work was supported by the National Natural Science Foundation of China (Grant Nos. 62125503 and 62261160388), the Key R&D Program of Hubei Province of China (Grant Nos. 2020BAB001 and 2021BAA024), the Key R&D Program of Guangdong Province (Grant No. 2018B030325002), the Science and Technology Innovation Commission of Shenzhen (Grant No. JCYJ202001091140 18750), the Open Projects Foundation (No. SKLD2201) of State Key Laboratory of Optical Fiber and Cable Manufacture Technology (YOFC), and the Innovation Project of Optics Valley Laboratory (Grant No. OVL2021BG004). The authors declare that there is no conflict of interest regarding the publication of this article.

Data Availability Statement

Data underlying the results presented in this paper are not publicly available at this time but may be obtained from the authors upon reasonable request.

References

1. R. Essiambre et al. "Capacity limits of optical fiber networks," *J. Lightwave Technol.* **28**, 662–701 (2010).
2. G. Li et al., "Space-division multiplexing: the next frontier in optical communication," *Adv. Opt. Photonics* **6**, 413–487 (2014).
3. D. J. Richardson, J. M. Fini, and L. E. Nelson, "Space-division multiplexing in optical fibres," *Nat. Photonics* **7**, 354–362 (2013).
4. N. Bozinovic et al., "Terabit-scale orbital angular momentum mode division multiplexing in fibers," *Science* **340**, 1545–1548 (2013).
5. J. Wang, "Advances in communications using optical vortices," *Photonics Res.* **4**, B14–B28 (2016).
6. J. Liu et al., "Direct fiber vector eigenmode multiplexing transmission seeded by integrated optical vortex emitters," *Light Sci. Appl.* **7**, 17148 (2018).
7. J. Wang and Y. Liang, "Generation and detection of structured light: a review," *Front. Phys.* **9**, 263 (2021).
8. J. Sakaguchi et al., "19-core fiber transmission of $19 \times 100 \times 172$ -Gb/s SDM-WDM-PDM-QPSK signals at 305Tb/s," in *Opt. Fiber Commun. Conf.*, Optical Society of America (2012), p. PDP5C.1.
9. K. Igarashi et al., "110.9-Tbit/s SDM transmission over 6,370 km using a full C-band seven-core EDFA," *Opt. Express* **21**, 18053–18060 (2013).
10. B. J. Puttnam et al., "2.15 Pb/s transmission using a 22 core homogeneous single-mode multi-core fiber and wideband optical comb," in *Eur. Conf. Opt. Commun. (ECOC)*, IEEE (2015).
11. D. Soma et al., "10.16-Peta-B/s dense SDM/WDM transmission over 6-mode 19-core fiber across the C+ L band," *J. Lightwave Technol.* **36**, 1362–1368 (2018).
12. G. Rademacher et al., "10.66 peta-bit/s transmission over a 38-core-three-mode fiber," in *Opt. Fiber Commun. Conf.* (Optical Society of America, 2020), paper Th3H.1.
13. D. Soma et al., "50.47-Tbit/s Standard cladding ultra-low-loss coupled 4-Core fiber transmission over 9,150 km," in *Opt. Fiber Commun. Conf.* (Optical Society of America, 2021) paper W7D.3.
14. Y. Liang et al., "Experimental demonstration of visualized multi-core fiber coupling alignment system for inter-core crosstalk measurement," *Opt. Lett.* **47**, 3071–3074 (2022).
15. A. V. Turukhin et al., "High capacity ultralong-haul power efficient transmission using 12-core fiber," *J. Lightwave Technol.* **35**, 1028–1032 (2017).

16. W. Klaus et al., "Free-space coupling optics for multicore fibers," *IEEE Photonics Technol. Lett.* **24**, 1902–1905 (2012).
 17. K. Igarashi et al., "Ultra-dense spatial-division-multiplexed optical fiber transmission over 6-mode 19-core fibers," *Opt. Express* **24**, 10213–10231 (2016).
 18. L. Gan et al., "Ultra-low crosstalk fused taper type fan-in/fan-out devices for multicore fibers," in *Opt. Fiber Commun. Conf.* (Optical Society of America, 2019), paper Th3D.3.
 19. B. Zhu et al., "Seven-core multicore fiber transmissions for passive optical network," *Opt. Express* **18**, 11117–11122 (2010).
 20. B. Li et al., "Experimental demonstration of large capacity WSDM optical access network with multicore fibers and advanced modulation formats," *Opt. Express* **23**, 10997–11006 (2015).
 21. K. Shikama et al., "Low-loss and low-mode-dependent-loss fan-in/fan-out device for 6-mode 19-core fiber," *J. Lightwave Technol.* **36**, 302–308 (2017).
 22. Y. Ding et al., "On-chip grating coupler array on the SOI platform for fan-in/fan-out of MCFs with low insertion loss and crosstalk," *Opt. Express* **23**, 3292–3298 (2015).
 23. J. L. P. Ruiz et al., "Compact dual-polarization silicon integrated couplers for multicore fibers," *Opt. Lett.* **46**, 3649–3652 (2021).
 24. S. Dwivedi et al., "Multicore fiber link with SiN integrated fan-out and InP photodiode array," *IEEE Photonics Technol. Lett.* **30**, 1921–1924 (2018).
 25. T. Watanabe, M. Hikita, and Y. Kokubun, "Laminated polymer waveguide fan-out device for uncoupled multi-core fibers," *Opt. Express* **20**, 26317–26325 (2012).
 26. D. Sukanuma and T. Ishigure, "Fan-in/out polymer optical waveguide for a multicore fiber fabricated using the Mosquito method," *Opt. Express* **23**, 1585–1593 (2015).
 27. R. R. Thomson et al., "Ultrafast-laser inscription of a three dimensional fan-out device for multicore fiber coupling applications," *Opt. Express* **15**, 11691–11697 (2007).
 28. R. R. Thomson et al., "Ultrafast laser inscription of a 121-waveguide fan-out for astrophotonics," *Opt. Lett.* **37**, 2331–2333 (2012).
 29. S. Gross and M. J. Withford, "Ultrafast-laser-inscribed 3D integrated photonics: challenges and emerging applications," *Nanophotonics* **4**, 332–352 (2015).
 30. A. Ross-Adams et al., "Enabling future fiber networks using integrated ultrafast laser-written multicore fiber fan-outs," in *Conf. Lasers and Electro-Opt. Pac. Rim (CLEO-PR)* (IEEE, 2020).
 31. G. Djogo et al., "Femtosecond laser additive and subtractive micro-processing: enabling a high-channel-density silica interposer for multicore fibre to silicon-photonics packaging," *Int. J. Extreme Manuf.* **1**, 45002 (2019).
 32. J. Cariñe et al., "Multi-core fiber integrated multi-port beam splitters for quantum information processing," *Optica* **7**, 542–550 (2020).
 33. B. Da Lio et al., "Stable transmission of high-dimensional quantum states over a 2-km multicore fiber," *IEEE J. Sel. Top. Quantum Electron.* **26**, 1–8 (2019).
 34. J. P. Moore and M. D. Rogge, "Shape sensing using multi-core fiber optic cable and parametric curve solutions," *Opt. Express* **20**, 2967–2973 (2012).
 35. P. S. Westbrook et al., "Continuous multicore optical fiber grating arrays for distributed sensing applications," *J. Lightwave Technol.* **35**, 1248–1252 (2017).
 36. J. Shin, B. T. Bosworth, and M. A. Foster, "Compressive fluorescence imaging using a multi-core fiber and spatially dependent scattering," *Opt. Lett.* **42**, 109–112 (2017).
 37. V. Tsvirkun et al., "Flexible lensless endoscope with a conformationally invariant multi-core fiber," *Optica* **6**, 1185–1189 (2019).
 38. M. Ams et al., "Slit beam shaping method for femtosecond laser direct-write fabrication of symmetric waveguides in bulk glasses," *Opt. Express* **13**, 5676–5681 (2005).
 39. S. Gómez et al., "Multidimensional entanglement generation with multicore optical fibers," *Phys. Rev. Appl.* **15**, 34024 (2021).
 40. R. R. Thomson et al., "Ultrafast laser inscription of an integrated photonic lantern," *Opt. Express* **19**, 5698–5705 (2011).
 41. H. Chen et al., "Design constraints of photonic-lantern spatial multiplexer based on laser-inscribed 3-D waveguide technology," *J. Lightwave Technol.* **33**, 1147–1154 (2015).
 42. R. G. Van Uden et al., "Ultra-high-density spatial division multiplexing with a few-mode multicore fibre," *Nat. Photonics* **8**, 865–870 (2014).
 43. P. Mitchell et al., "57 channel (19× 3) spatial multiplexer fabricated using direct laser inscription," in *Opt. Fiber Commun. Conf.* (Optical Society of America, 2014), paper M3K.5.
 44. S. Rommel et al., "Characterization of a fiber-coupled 36-core 3-mode photonic lantern spatial multiplexer," in *Photonic Networks and Devices* (Optica Publishing Group, 2017), paper NeW3B. 2.
 45. N. Riesen et al., "Monolithic mode-selective few-mode multicore fiber multiplexers," *Sci. Rep.* **7**, 1–9 (2017).
- Yize Liang** received his BS degree from Huazhong University of Science and Technology in 2018. Currently, he is pursuing his PhD at Wuhan National Laboratory for Optoelectronics and School of Optical and Electronic Information at Huazhong University of Science and Technology. His research interests include structured light and multimode fibers.
- Chengkun Cai** received his BS degree from Huazhong University of Science and Technology in 2017. Currently, he is pursuing his PhD at Wuhan National Laboratory for Optoelectronics and School of Optical and Electronic Information at Huazhong University of Science and Technology. His research interest includes femtosecond laser fabrication.
- Kangrui Wang** received his BS degree from Huazhong University of Science and Technology in 2022. Currently, he is pursuing his PhD at Wuhan National Laboratory for Optoelectronics and School of Optical and Electronic Information at Huazhong University of Science and Technology. His research interest includes femtosecond laser direct writing.
- Xiaokang Lian** received his PhD in optical engineering from Technological University Dublin, Dublin, Ireland, in 2021. Currently, he is working as a postdoctoral research associate in Multi-Dimensional Photonics Laboratory at the Wuhan National Laboratory for Optoelectronics, Huazhong University of Science and Technology, Wuhan, China.
- Jue Wang** is pursuing his PhD at Wuhan National Laboratory for Optoelectronics and School of Optical and Electronic Information at Huazhong University of Science and Technology. His research interests include femtosecond laser micron-nano fabrication and optical devices.
- Jinfeng Liu** received his BS degree from Huazhong University of Science and Technology in 2022. Currently, he is pursuing his PhD at Wuhan National Laboratory for Optoelectronics at Huazhong University of Science and Technology. His research interest includes light field manipulation.
- Lei Shen** received his PhD in experimental mechanics from Huazhong University of Science and Technology. Currently, he is working as a senior specialist of Yangtze Optical Fiber and Cable Joint Stock Limited Company, Wuhan, Hubei province. His research interests include the design, fabrication, and measurement of new optical fiber and cable products for outside plant, indoor, and FTTH applications.
- Jian Wang** received his PhD in physical electronics from Wuhan National Laboratory for Optoelectronics, Huazhong University of Science and Technology, Wuhan, China, in 2008. He worked as a post-doctoral research associate in the Optical Communications Laboratory,

University of Southern California, Los Angeles, California, United States, from 2009 to 2011. Currently, he is working as a professor at Wuhan National Laboratory for Optoelectronics, Huazhong University of Science and Technology. He is the vice director of Wuhan National Laboratory for Optoelectronics, Huazhong University of Science and Technology. He leads the Multi-Dimensional Photonics Laboratory. His research interests include optical communications, optical signal processing, silicon photonics, photonic integration, orbital angular momentum, and structured light. He has published more than 260 refereed

international journal papers in *Science*, *Science Advances*, *Nature Photonics*, *Nature Communications*, *Light: Science and Applications*, *Physical Review Letters*, *Optica*, *Laser and Photonics Reviews*, *Research*, *Photonix*, *Advanced Photonics*, *ACS Photonics*, etc. He has authored and co-authored more than 150 international conference papers on OFC, ECOC, CLEO, etc. He has also given more than 110 tutorial/keynote/invited talks at international conferences including an invited talk at OFC2014 and tutorial talk at OFC2016. He is currently an OPTICA Fellow and SPIE Fellow.